Superconducting proximity effect in quantum wires without time-reversal symmetry

M. A. Skvortsov,[1,2] P. M. Ostrovsky,[1,3] D. A. Ivanov,[4,5] and Ya. V. Fominov[1,2]
[1]*L. D. Landau Institute for Theoretical Physics, 142432 Chernogolovka, Russia*
[2]*Moscow Institute of Physics and Technology, 141700 Moscow, Russia*
[3]*Max Planck Institute for Solid State Research, Heisenbergstrasse 1, 70569 Stuttgart, Germany*
[4]*Institute for Theoretical Physics, ETH Zürich, 8093 Zürich, Switzerland*
[5]*Institute for Theoretical Physics, University of Zürich, 8057 Zürich, Switzerland*
(Received 7 November 2012; published 4 March 2013)

We study the superconducting proximity effect in a quantum wire with broken time-reversal (TR) symmetry connected to a conventional superconductor. We consider the situation of a strong TR-symmetry breaking, so that Cooper pairs entering the wire from the superconductor are immediately destroyed. Nevertheless, some traces of the proximity effect survive: for example, the local electronic density of states (LDOS) is influenced by the proximity to the superconductor, provided that localization effects are taken into account. With the help of the supersymmetric sigma model, we calculate the average LDOS in such a system. The LDOS in the wire is strongly modified close to the interface with the superconductor at energies near the Fermi level. The relevant distances from the interface are of the order of the localization length, and the size of the energy window around the Fermi level is of the order of the mean level spacing at the localization length. Remarkably, the sign of the effect is sensitive to the way the TR symmetry is broken: In the spin-symmetric case (orbital magnetic field), the LDOS is depleted near the Fermi energy, whereas for the broken spin symmetry (magnetic impurities), the LDOS at the Fermi energy is enhanced.

DOI: 10.1103/PhysRevB.87.104502 PACS number(s): 74.45.+c, 73.20.Fz, 73.21.Hb

I. INTRODUCTION

Proximity effect in normal–superconducting structures is a phenomenon of induced superconducting correlations in the normal metal (N) in an electric contact with a superconductor (S).[1] Such correlations arise due to Andreev reflections at the NS interface: an electron from the N part reflects as a hole by emitting a Cooper pair into the S part.[2] The extent of such proximity correlations is determined by the structure and geometry of the N part: in a small N grain, the correlations are uniform over its volume, while in a large N contact the proximity correlations extend over some distance determined by the energy of the electrons relative to the Fermi energy.[3,4]

One of the signatures of the proximity effect is the modification of the local electronic density of states (LDOS) in the N part. Such a modification is most pronounced in the case of chaotic electron dynamics in the N part, when a so-called "minigap" is formed in the density of states.[5] The size of the minigap can be estimated as $\min(\Delta, 1/\tau_{\mathrm{esc}})$, where Δ is the superconducting gap and τ_{esc} is the time required for an electron in the N region to establish a contact with the superconductor[6,7] (hereafter we assume $\hbar = 1$). In particular, for a long diffusive wire (with its length L exceeding the superconducting coherence length) and transparent NS interface, the minigap is of the order of the Thouless energy,[8]

$$E_{\mathrm{Th}} = D/L^2, \tag{1}$$

where D is the diffusion coefficient.

The proximity effect is sensitive to the time-reversal (TR) symmetry in the N part, which is necessary for superconducting correlations. If the TR symmetry is broken (e.g., by a strong magnetic field or by magnetic impurities), then the conventional quasiclassical theory predicts that no proximity effect can survive beyond the distance over which the TR symmetry is broken.[4]

However, this quasiclassical description is known to be incomplete. The most prominent example of a proximity effect in the absence of the TR symmetry is the random-matrix theory (RMT): indeed, in superconducting symmetry classes with broken TR symmetry, the density of states is modified in the energy window of the order of the interlevel spacing around the Fermi energy.[9] In extended systems, the perturbative modes (diffusons and possibly cooperons, depending on the symmetry) responsible for the proximity effect beyond the quasiclassical approximation have been identified in Refs. 9 and 10. The interplay between such mesoscopic fluctuations and localization effects was studied in various superconducting and chiral symmetry classes in Refs. 11–14.

In our present paper, we consider another example of a nonquasiclassical superconducting proximity effect in disordered quantum wires with broken TR symmetry. Under the assumption of a quantum coherence, the relevant length and energy scales in such systems are determined by the Anderson localization.[15] The length scale at which the LDOS is modified due to the proximity effect is given by the localization length ξ. The corresponding energy scale Δ_ξ is given by the level spacing between states at the length ξ. In one-dimensional geometry,[16]

$$\Delta_\xi = D/\xi^2. \tag{2}$$

We illustrate this qualitative picture with an explicit calculation in the model of a quantum wire with a large number of conducting channels. Namely, we consider such a wire (of a finite length L) with a broken TR symmetry in a contact with a superconductor (Fig. 1). Using the method of the nonlinear supersymmetric σ model,[17,18] in conjunction with recent exact results for localization in quasi-one-dimensional unitary wires,[19–21] we calculate the average LDOS as a function of

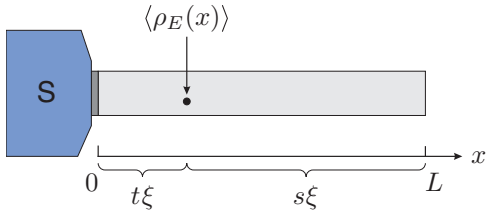

FIG. 1. (Color online) Quantum wire of length L coupled to a massive superconductor at $x = 0$. We calculate the average local density of states $\langle \rho_E(x) \rangle$ for an arbitrary relation between x, L, and the localization length ξ. The dimensionless distances t and s are used in Eq. (13).

energy and coordinate along the wire in different limiting cases.

A remarkable detail of our analysis is the two different ways of breaking the TR symmetry. Namely, it may be broken either *without* breaking the spin-rotational symmetry (e.g., by a strong magnetic field inducing a TR-symmetry-breaking vector potential, but only a negligible Zeeman field) or *with* breaking the spin-rotational symmetry (e.g., by including magnetic impurities coupled to the spins of electrons). These two possibilities correspond to different symmetry classes in the RMT classification (C and D, respectively)[9] and exhibit quite different types of the proximity effect. First, while in class C the LDOS is suppressed at low energies and at short distances, in class D it is enhanced (similar to the RMT results). Second, in long wires ($L \gg \xi$) at small energies ($E \ll \Delta_\xi$), the proximity effect extends to the Mott length scale[22]

$$L_M = 2\xi \ \ln(\Delta_\xi / E) \tag{3}$$

in class C, while only to the localization length ξ in class D (Fig. 6). Such a behavior is related to the presence (absence) of repulsion between an energy level and its mirror counterpart in the symmetry class C (D) and is discussed in Sec. VI.

The paper is organized as follows. In Sec. II we explain the relation of the proximity effect in the absence of the TR symmetry to Anderson localization. Evaluation of the LDOS for a quasi-one-dimensional wire with the broken TR symmetry is reduced to the unitary σ model in Sec. III, and its exact solution is presented in Sec. IV. Resulting expressions for the LDOS in various limiting cases are derived in Sec. V. Our findings are summarized in Sec. VI. Technical details are relegated to several Appendices.

II. PROXIMITY EFFECT WITHOUT TIME-REVERSAL SYMMETRY: ROLE OF LOCALIZATION

In a diffusive system (without TR symmetry breaking), the superconducting proximity effect is described by the quasiclassical Usadel equation.[23] For a given energy, E, superconducting correlations decay into the normal region at the diffusive length scale

$$L_E = \sqrt{D/E}\,. \tag{4}$$

The TR symmetry is needed to establish particle-hole correlations (the soft "cooperon" modes[24]) in the wire. In this paper, we consider the opposite situation: the proximity effect in the case of the broken TR symmetry. It may be broken in two different ways: by an external magnetic field (symmetry class C) or by magnetic impurities (symmetry class D). In both cases, the spectrum of the cooperon modes acquires a gap leading to their exponential decay at some characteristic scale L_c. This scale is set either by the magnetic length or by the spin diffusion length. As long as L_c is shorter than L_E (at sufficiently low energies and, e.g., strong magnetic field), superconductive coherence brought into the normal metal by cooperon modes exists only in a thin layer of length L_c near the boundary, decaying exponentially at larger distances.

This exponential decay of superconductive correlations at $L \gg L_c$ follows from the Usadel equation.[4] The latter is an effective tool for nonperturbative summation of treelike diagrams[25] but neglects loop corrections responsible for quantum localization. We will show below that these corrections, though suppressed as $1/N$ ($N \gg 1$ is the number of the conducting channels in the wire), give rise to the proximity effect in the absence of the TR symmetry.

Localization length in a N wire with the broken TR symmetry is given by[18,26,27]

$$\xi = 2\pi \nu A D \sim N l. \tag{5}$$

Here A is the wire cross section, l is the mean-free path, and ν is the bulk density of states, whose definition depends on spin degeneracy as follows.

(1) In class C (an external magnetic field), the spin symmetry is preserved, and hence all electron states are doubly degenerate. In this case, the density of states ν [in Eq. (5) and throughout the paper] is defined per spin projection.

(2) In class D (magnetic impurities), the disorder mixes spin components, and ν is defined as the total density of states including spin.

Relation between the proximity effect in the absence of the TR symmetry and localization can be visualized diagrammatically in the limit of poor transparency of the SN interface when all transmission coefficients of the barrier are small, $T \ll 1$. Then the influence of the superconductor can be treated perturbatively. In the TR-symmetric case, the leading process is shown in Fig. 2(a): a Cooper pair tunnels at a point $\mathbf{r}_1$, propagates to the observation point $\mathbf{r}$, and returns back to the superconductor at a point $\mathbf{r}_2$. Integrations over $\mathbf{r}_{1,2}$

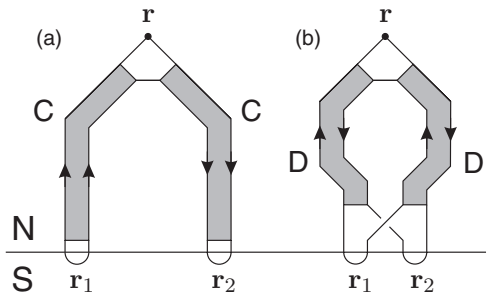

FIG. 2. Diagrams for the proximity-induced correction to the local density of states $\langle \rho_E(\mathbf{r}) \rangle$ to the lowest order in the tunneling transparency of the SN interface: (a) TR-symmetric case, when Cooper pairs independently tunnel at $\mathbf{r}_1$ and $\mathbf{r}_2$ and propagate in the N part as cooperons (shadowed); (b) broken TR-symmetry case, when Cooper pairs tunnel at $\mathbf{r}_1 \approx \mathbf{r}_2$, propagating further as two diffusons (shadowed).

taken across the wire section are independent, and the resulting correction to the LDOS $\langle\delta\rho_E(\mathbf{r})\rangle$ is proportional to N^2T^2. In the case of broken TR symmetry, cooperons are suppressed, but the LDOS is still affected by the process depicted in Fig. 2(b): a tunneling Cooper pair needs to be converted to a pair of diffusons which can reach the observation point. For such a process, the tunneling coordinates nearly coincide, $\mathbf{r}_1 \approx \mathbf{r}_2$, and integration over them brings the first power of the wire cross section: $\langle\delta\rho_E(\mathbf{r})\rangle \propto NT^2$. At the same time we see that the spatial behavior of the LDOS corrections (a) and (b) are identical: both decay at the scale L_E. The $1/N \propto 1/\xi$ suppression of the LDOS correction in the absence of the TR symmetry is reminiscent of localization and is related to one-loop structure of the diagram (b), contrary to the treelike diagram (a) accounted for by the Usadel equation.

III. REDUCTION TO THE UNITARY σ MODEL

Electronic states in superconducting systems are described with the help of the Bogolyubov–de Gennes (BdG) Hamiltonian, which acts as a matrix in the Nambu space:

$$\hat{\mathcal{H}}_{\mathrm{BdG}} = \begin{pmatrix} \mathcal{H} & \Delta \\ \Delta^* & -\Theta\mathcal{H}^*\Theta^{-1} \end{pmatrix}, \tag{6}$$

where $\mathcal{H}$ is the single-particle Hamiltonian, Δ is the order parameter field, and Θ is a unitary matrix that defines the time-reversal operation: $\psi \mapsto \Theta\psi^*$. If the spin symmetry is preserved (class C), we write the BdG Hamiltonian (6) for one spin projection (e.g., spin-up electrons and spin-down holes) and fix $\Theta = 1$. On the contrary, in class D, when the single-particle spin dynamics is nontrivial, we include both spin projections and put $\Theta = is_y$ (the Pauli matrix in the spin space). Thus, in class D, the dimension of the Hamiltonian (6) is two times larger than in class C.

We define the quasiparticle LDOS normalized to the bulk value as

$$\rho_E(\mathbf{r}) = -\frac{1}{2\pi\nu}\,\mathrm{Im}\,\mathrm{tr}\,\mathcal{G}_E^R(\mathbf{r},\mathbf{r}). \tag{7}$$

It is expressed in terms of the retarded Green function of the BdG Hamiltonian (6),

$$\mathcal{G}_E^R = (E - \hat{\mathcal{H}}_{\mathrm{BdG}} + i0)^{-1}. \tag{8}$$

Note that the definition of ν in Eq. (7) is different in the C and D classes (see Sec. II), which is consistent with the difference in the dimensionality of $\hat{\mathcal{H}}_{\mathrm{BdG}}$.

In a field-theoretical language,[10,28–31] disorder averaging of $\rho_E(\mathbf{r})$ is performed by representing $\mathcal{G}_E^R$ as a supersymmetric functional integral and following the standard line of the σ-model derivation.[18] The details of the derivation are presented in Appendix A, and below we summarize the results.

In the normal part ($\Delta = 0$) of a hybrid NS system, the Nambu-Gor'kov Green function $\mathcal{G}_E^R$ essentially involves a pair of the retarded and advanced normal-metal Green functions with opposite energies, G_E^R and G_{-E}^A, which get coupled due to Andreev reflection off the superconducting order parameter. Therefore, the σ model for $\langle\mathcal{G}_E^R\rangle$ in the normal region of a NS system can be exactly rewritten in terms of Evetov's σ model for the product $\langle G_E^R G_{-E}^A\rangle$. This relation has been recently demonstrated in Ref. 32, where an explicit mapping between the two models was constructed. In our problem, $\langle\rho_E(\mathbf{r})\rangle$ may be calculated in terms of the usual Efetov's σ model written for the normal wire, but supplemented with a boundary condition at the NS interface responsible for Andreev reflections.

The TR symmetry in the wire can be broken either by the orbital magnetic field or by magnetic impurities. In the former case each level is double degenerate due to the spin symmetry, whereas in the latter case this Kramers degeneracy is lifted. For sufficiently strong symmetry breaking[33] (or at length scale larger than the length L_c associated with the TR symmetry breaking) models IIa and IIb in Efetov's classification[18] are realized. In both cases, the cooperon degrees of freedom are frozen out, and the resulting σ model is written in terms of a 4×4 supermatrix acting in the Fermi-Bose (FB) and retarded-advanced (RA) spaces.

For a normal metal, the models IIa and IIb are mathematically equivalent (unitary σ model). This is not the case for the normal part of a hybrid system, since the form of the effective boundary condition at the NS interface is sensitive to the way the TR symmetry is broken. In the presence of Andreev scattering, the models IIa and IIb correspond to the symmetry classes C and D in the classification of Ref. 9.

Thus, in the limit of strongly broken TR symmetry, the proximity effect in the normal part of an NS system is described by Efetov's unitary σ model. The average (normalized) LDOS is given by the functional integral over the normal-metal region:

$$\langle\rho_E(\mathbf{r})\rangle = \frac{1}{4}\,\mathrm{Re}\int \mathrm{str}(k\Lambda Q(\mathbf{r}))e^{-S[Q]-S_\Gamma[Q]}d[Q]. \tag{9}$$

The action of the model is separated into the bulk diffusive part $S[Q]$ and the boundary term $S_\Gamma[Q]$, derived in Appendix A. The bulk action has the standard form for the unitary class σ model,

$$S = \frac{\pi\nu}{4}\int d\mathbf{r}\ \mathrm{str}[D(\nabla Q)^2 + 4iE\Lambda Q], \tag{10}$$

with the 4×4 supermatrix Q acting in the FB and RA spaces. The matrix $\Lambda = \sigma_z^{\mathrm{RA}}$ is the metallic saddle point, and the supersymmetry breaking matrix $k = \sigma_z^{\mathrm{FB}}$ (we follow notations of Ref. 18). As before, D is the diffusion coefficient and ν is the density of states at the Fermi level per one spin projection if the spin is conserved (class C) and including both spin projections in the case of broken spin symmetry (class D).

The boundary action is derived in Appendix A (see also Ref. 32). Throughout the paper, we assume for simplicity that the superconducting gap Δ in the S part is large. The precise condition on Δ is formulated in Eq. (A16). Under this assumption, the boundary action simplifies to the form

$$S_\Gamma = -\frac{1}{2}\sum_i \mathrm{str}\ln[1 - e^{-4\beta_i}Q(0)\Xi Q^T(0)\Xi^T]. \tag{11}$$

Here the parameters β_i are related to the transmission coefficients at the SN interface: $T_i = 1/\cosh^2\beta_i$, with i labeling open channels. In the case of conserved spin (class C), the channels are double degenerate but the index i counts them only once. With broken spin symmetry (class D), this degeneracy is lifted. In both cases, the normal-state conductance can be written as a product $G_0 g_N$, where $g_N = \sum_i T_i$, and the

conductance quantum is defined as $G_0 = 2e^2/h$ for class C and $G_0 = e^2/h$ for class D.

The main ingredient which distinguishes between the symmetry classes C and D is the matrix Ξ entering Eq. (11). For class C it has been derived in Ref. 32, and derivation for both classes is presented in Appendix A:

$$\text{class C}: \quad \Xi = \begin{pmatrix} i\sigma_y^{\mathrm{RA}} & 0 \\ 0 & \sigma_x^{\mathrm{RA}} \end{pmatrix}_{\mathrm{FB}}, \tag{12a}$$

$$\text{class D}: \quad \Xi = \begin{pmatrix} \sigma_x^{\mathrm{RA}} & 0 \\ 0 & i\sigma_y^{\mathrm{RA}} \end{pmatrix}_{\mathrm{FB}}. \tag{12b}$$

The matrix Ξ has a nontrivial structure in the superspace, which is the mathematical reason why Eq. (9) results in a nontrivial LDOS.

Note that the matrix Ξ does not belong to the standard unitary manifold for Q matrices: it does not obey the condition $\Xi^2 = 1$ [in the F (B) sector for class C (D), respectively]. One finds that the saddle-point solution for the action $S[Q] + S_\Gamma[Q]$ is simply $Q(\mathbf{r}) = \Lambda$, leading to the metallic density of states, $\rho(\mathbf{r}) = 1$, indicating no proximity effect at the level of the Usadel equation. However, proximity effect absent in the quasiclassical approximation will manifest itself once fluctuations around Λ are taken into account. The same fluctuations are responsible for localization. Thus the superconducting proximity effect in a normal metal with broken TR symmetry is inevitably related to localization, leading to strong modification of the LDOS near the SN interface at energies $E \lesssim \Delta_\xi$ and length scales $x \lesssim \xi$.

IV. ANALYTIC SOLUTION FOR QUASI-1D WIRES

Here we apply the general framework described in the previous section in order to calculate the average LDOS, $\langle \rho_E(x) \rangle$, in a finite quasi-one-dimensional wire of length L coupled to a superconductor at $x = 0$; see Fig. 1. We will work in the limit of large Δ, which is spelled out in Eq. (A16) of Appendix A, and assume that the TR symmetry in the wire is completely broken.

The one-dimensional σ model (9) can be solved exactly by mapping onto effective quantum mechanics,[27] with the x coordinate playing the role of the imaginary time. In this formalism, evaluation of the functional integral (9) is reduced to solving Schrödinger equations for the wave functions $\Psi(Q)$ on the σ-model manifold. This technical procedure described in Appendix A leaves us with the object $\Psi(\lambda_F, \lambda_B)$ depending only on the "eigenvalues" λ_F and λ_B of the Q matrix.

The main ingredient for calculation of $\langle \rho_E(x) \rangle$ is the wave function $\Psi(\lambda_F, \lambda_B; t, s)$, which accounts for coherent motion of the electron and hole in the wire. It can be obtained by successive application of two evolution operators on unity (corresponds to open boundary conditions at the free end of the wire):

$$\Psi(\lambda_F, \lambda_B; t, s) = e^{-2\tilde{H}t} e^{-2Hs} \circ 1, \tag{13}$$

where (see Fig. 1)

$$t = x/\xi, \quad s = (L - x)/\xi. \tag{14}$$

The Hamiltonians $\tilde{H}$ and H govern imaginary-time evolution at the segments $[0, x]$ and $[x, L]$, respectively. They have the form[27]

$$H = -\frac{(\lambda_B - \lambda_F)^2}{2} \left[\frac{\partial}{\partial \lambda_F} \frac{1 - \lambda_F^2}{(\lambda_B - \lambda_F)^2} \frac{\partial}{\partial \lambda_F} + \frac{\partial}{\partial \lambda_B} \frac{\lambda_B^2 - 1}{(\lambda_B - \lambda_F)^2} \frac{\partial}{\partial \lambda_B} \right] + \frac{\kappa^2}{16} (\lambda_B - \lambda_F) \tag{15}$$

and[20,21]

$$\tilde{H} = (\lambda_B - \lambda_F)^{-1} H (\lambda_B - \lambda_F) = \tilde{H}_B + \tilde{H}_F, \tag{16}$$

with

$$\tilde{H}_B = -\frac{1}{2} \frac{\partial}{\partial \lambda_B} \left(\lambda_B^2 - 1 \right) \frac{\partial}{\partial \lambda_B} + \frac{\kappa^2}{16} \lambda_B, \tag{17a}$$

$$\tilde{H}_F = -\frac{1}{2} \frac{\partial}{\partial \lambda_F} \left(1 - \lambda_F^2 \right) \frac{\partial}{\partial \lambda_F} - \frac{\kappa^2}{16} \lambda_F, \tag{17b}$$

where the dimensionless quantity κ stands for

$$\kappa^2 = -\frac{8iE}{\Delta_\xi} \tag{18}$$

[it is consistent with the notations of Refs. 19 and 21, with the frequency $\omega = E - (-E) = 2E$].

Unfortunately, the function $\Psi(\lambda_F, \lambda_B; t, s)$ cannot be generally obtained in a closed form. The only exception is the zero mode of the Hamiltonian H, $\Psi_0(\lambda_F, \lambda_B) \equiv \Psi(\lambda_F, \lambda_B; 0, \infty)$, given by[19]

$$\Psi_0(\lambda_F, \lambda_B) = I_0(q) p K_1(p) + q I_1(q) K_0(p), \tag{19}$$

where

$$p = \kappa \sqrt{(\lambda_B + 1)/2}, \quad q = \kappa \sqrt{(\lambda_F + 1)/2}, \tag{20}$$

and I_n and K_n are the modified Bessel functions.

The function $\Psi(\lambda_F, \lambda_B; t, s)$ should be finally integrated over $Q(0)$ with the weight $e^{-S_\Gamma[Q]}$ in order to obtain $\langle \rho_E(x) \rangle$. At this stage calculations for the symmetry classes C and D are different due to a different form of the superconducting matrix (12).

A. General expression for class C

For the symmetry class C, calculations presented in Appendix B lead to the following exact expression:

$$\langle \rho_E(x) \rangle = 1 + \frac{1}{2} \operatorname{Re} \int_{-1}^{1} d\lambda_F \int_{1}^{\infty} d\lambda_B \times \frac{\partial e^{-S_0^{\mathrm{C}}(\lambda_B)}}{\partial \lambda_B} \Psi(\lambda_F, \lambda_B; t, s). \tag{21}$$

Parameters of the SN interface are encoded in the boundary action:

$$S_0^{\mathrm{C}}(\lambda_B) = \frac{1}{2} \sum_i \ln \left[1 + \mathcal{T}_i \left(\lambda_B^2 - 1 \right) \right], \tag{22}$$

where

$$\mathcal{T}_i = \frac{T_i^2}{(2 - T_i)^2} \tag{23}$$

is the Andreev transmission of the ith channel.[34]

The boundary action (22) suppresses fluctuation of the bosonic variable λ_B. The strength of the coupling to the

superconductor is characterized by the dimensionless [in units of G_0 defined below Eq. (11)] Andreev conductance of the interface,

$$g_A = 2\sum_i \mathcal{T}_i. \tag{24}$$

In the limit of $g_A \gg 1$, the integral over λ_B in Eq. (21) comes from $\lambda_B - 1 \lesssim 1/g_A$. If $\Psi(\lambda_F,\lambda_B;t,s)$ is a slow function of λ_B in this region, then Eq. (21) simplifies to

$$\langle\rho_E(x)\rangle = 1 - \frac{1}{2}\,\mathrm{Re}\int_{-1}^{1} d\lambda_F \Psi(\lambda_F,1;t,s). \tag{25}$$

As we will see below, approximation (25) applies if

$$g_A \gg 1 \quad \text{and} \quad g_A \gg \min(\xi/L_E, E/\delta), \tag{26}$$

where $\delta = (2\nu AL)^{-1}$ is the mean level spacing in the wire.

B. General expression for class D

In close analogy with Eq. (21), calculations in Appendix B lead for the symmetry class D:

$$\langle\rho_E(x)\rangle = 1 + \frac{1}{2}\,\mathrm{Re}\int_{-1}^{1} d\lambda_F \int_1^{\infty} d\lambda_B \times \frac{\partial e^{-S_0^{\mathrm{D}}(\lambda_F)}}{\partial\lambda_F}\Psi(\lambda_F,\lambda_B;t,s), \tag{27}$$

with the boundary action

$$S_0^{\mathrm{D}}(\lambda_F) = -\frac{1}{2}\sum_i \ln\left[1 - \mathcal{T}_i\left(1-\lambda_F^2\right)\right]. \tag{28}$$

For large g_A [Eq. (26)], λ_F is pinned to ± 1 and we obtain

$$\langle\rho_E(x)\rangle = 1 + \frac{1}{2}\,\mathrm{Re}\int_1^{\infty} d\lambda_B[\Psi(1,\lambda_B;t,s) - \Psi(-1,\lambda_B;t,s)]. \tag{29}$$

V. RESULTS

Here we analyze the general expressions (21) and (27) in various regions of the system parameters, schematically shown in Fig. 3. We will be mainly interested in the limit $g_A \to \infty$ [Eq. (26)] when the LDOS is given by Eqs. (25) and (29), and present the result for an arbitrary g_A only in the perturbative regime discussed in Sec. V B.

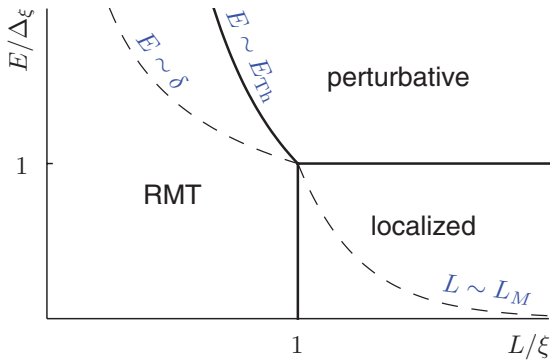

FIG. 3. (Color online) Regions of different behavior of the average LDOS in the coordinates L/ξ and E/Δ_ξ.

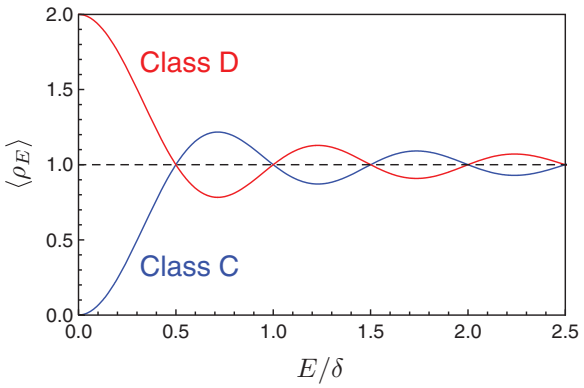

FIG. 4. (Color online) Energy dependence of the RMT density of states for the symmetry classes C and D.

A. Random-matrix regime ($L \ll \xi$ and $E \ll E_{\mathrm{Th}}$)

We start the analysis of the general expression (25) for the LDOS with the simplest case of short wires, $L \ll \xi$. In the limit of $E \ll E_{\mathrm{Th}}$, electrons have enough time to explore the whole available space and one should recover the RMT statistics. In this case, one can neglect the terms with derivatives in the Hamiltonians: $H \approx \tilde{H} \approx (\kappa^2/16)(\lambda_B - \lambda_F)$, and one simply gets

$$\Psi(\lambda_F,\lambda_B;t,s) = e^{-(\kappa^2/8)(\lambda_B-\lambda_F)(L/\xi)}, \tag{30}$$

independently of x. Substituting into Eqs. (25) and (29) one readily recovers the RMT results for the symmetry classes C (minus sign) and D (plus sign):[9]

$$\langle\rho_E(x)\rangle = 1 \mp \frac{\sin(2\pi E/\delta)}{(2\pi E/\delta)}, \tag{31}$$

with the mean level spacing

$$\delta = (2\nu AL)^{-1} \tag{32}$$

(this definition of the level spacing takes into account both electron and hole states; hence it contains an additional factor 1/2). Energy dependence of the RMT density of states is shown in Fig. 4.

The gradient terms in the σ model may be taken into account perturbatively, which results in a position-dependent correction to the RMT density of states (31):

$$\langle\delta\rho_E(x)\rangle = \pm\frac{L}{\xi}\left\{\left[\frac{1}{3} - \left(1-\frac{x}{L}\right)^2\right]\left(1 \mp \frac{\sin(2\pi E/\delta)}{2\pi E/\delta}\right) + \frac{1 \mp \cos(2\pi E/\delta)}{3} + O(L/\xi) + O(E/E_{\mathrm{Th}})\right\}, \tag{33}$$

with the upper (lower) signs corresponding to the symmetry class C (D). Note that in the symmetry class C both the main result (31) and the correction (33) vanish at zero energy. The gradient terms in the Hamiltonians H and $\tilde{H}$ become significant if the length of the wire L exceeds ξ or at high energies $E \gtrsim E_{\mathrm{Th}}$. This establishes the boundaries of the RMT regime; see Fig. 3.

B. Perturbative regime ($E \gg E_{\rm Th}, \Delta_\xi$)

For $E \gg \max(E_{\rm Th}, \Delta_\xi)$, the LDOS is close to 1 everywhere in the wire, with the difference $\langle \rho_E(x) \rangle - 1$ decaying at the length scale L_E from the SN boundary. In this case only small deviations of λ_F and λ_B from 1 are important. Then the Hamiltonians H and $\tilde{H}$ can be simplified in the vicinity of $\lambda_F = \lambda_B = 1$ ("north pole" of the fermionic sphere) yielding an effective linear oscillator model. In this approximation, the wave function (13) takes the following form:

$$\Psi(\lambda_F,\lambda_B;t,s) = \frac{\cosh^2(\kappa s/2)}{\cosh^2(\kappa(t+s)/2)} \times \exp\left(-\frac{\kappa(\lambda_B-\lambda_F)}{4}\tanh\frac{\kappa(t+s)}{2}\right). \tag{34}$$

The density of states for the two symmetry classes then follows from Eqs. (21) and (27), where only small deviations of λ_F and λ_B from 1 are important. In this limit, the boundary actions (22) and (28) take the form $S_0^{\rm C}(\lambda_B) = (g_A/2)(\lambda_B - 1)$ and $S_0^{\rm D}(\lambda_F) = (g_A/2)(1-\lambda_F)$. Integrating over $1-\lambda_F$ and $\lambda_B - 1$, we obtain

$$\langle \rho_E(x) \rangle = 1 \mp 4\,{\rm Re}\,\frac{\cosh^2 \kappa s/2}{\kappa \sinh \kappa(t+s)} \times \frac{g_A}{g_A + (\kappa/2)\tanh(\kappa(t+s)/2)}. \tag{35}$$

As in Eq. (31), the minus (plus) sign corresponds to the symmetry class C (D).

Modification of the metallic LDOS by the proximity effect is maximal for good SN contacts with $g_A \gg g_N(L_E)$, where $g_N(L_E) = \xi/L_E = \sqrt{E/\Delta_\xi}$ is the normal-state conductance of the wire of length L_E. In this case, the second factor in the correction (35) may be approximated by one, and the result (in the physical units) reads

$$\langle \rho_E(x) \rangle = 1 \mp \frac{2L_E}{\xi}\,{\rm Re}\,\frac{\cosh^2[(1-i)(L-x)/L_E]}{(1-i)\sinh[2(1-i)L/L_E]}. \tag{36}$$

In the particular case of an infinite wire, Eq. (36) simplifies to

$$\langle \rho_E(x) \rangle = 1 \mp \frac{L_E}{\sqrt{2}\,\xi}\,e^{-2x/L_E}\cos\left(\frac{2x}{L_E}+\frac{\pi}{4}\right). \tag{37}$$

[Similar simplifications are also possible in the opposite limit $g_A \ll g_N(L_E)$: in that case, the perturbative corrections in Eqs. (36) and (37) get multiplied by g_A and correspond to the diagram in Fig. 2(b).] This result agrees with our argument in Sec. II: the proximity effect extends to the normal region at the length scale L_E (just like in the conventional Usadel equation), but its magnitude is small as $L_E/\xi \ll 1$ (in the perturbative regime).

Note that our perturbative calculation gives only the contribution to the LDOS from the vicinity of the north pole of the fermionic sphere ($\lambda_F = \lambda_B = 1$). In fact, the expressions (34)–(36) provide a valid perturbative treatment of the north-pole contribution at energies $E \gg \max(\delta, \Delta_\xi)$. In particular, in the window $\delta \ll E \ll E_{\rm Th}$, the north-pole contribution (36) reproduces the nonoscillating parts of the RMT result (31) and (33).

The south pole of the fermionic sphere ($\lambda_F = -1, \lambda_B = 1$) is an alternative saddle point of the action, which is responsible for the terms oscillating in energy with the period δ in the RMT [see, e.g., Eqs. (31) and (33)].[35] At energies $E \gg E_{\rm Th}$, its contribution is exponentially suppressed, and therefore it was neglected in our perturbative calculation. However, at energies $E \lesssim E_{\rm Th}$, the south-pole contribution exceeds, by absolute value, the correction to unity in Eq. (36). Note that at $E \gg \max(\delta, \Delta_\xi)$ the south-pole contribution may also be found in a perturbative scheme analogous to the one above, but expanding around the south pole instead. We do not report this calculation here, but only remark that, within the window $\delta \ll E \ll E_{\rm Th}$, it can reproduce the oscillating terms in the RMT expansion (31) and (33). In other words, this energy window represents an overlap between the RMT and perturbative approaches (if the south pole is taken into account).

C. Localized regime ($L \gg \xi$ and $E \ll \Delta_\xi$)

Finally, we turn to the limit of long wires, $L \gg \xi$. Here the difference between the symmetry classes C and D becomes more pronounced than just the sign in Eqs. (31) and (35), and they require separate considerations. As in subsection A, our results in this section are restricted to the "good contact" limit $g_A \gg 1$ [see Eq. (26)].

1. Symmetry class C

Using Eq. (19) for the zero mode, one immediately obtains an exact expression for the energy dependence of the LDOS at the SN interface for the semi-infinite wire:

$$\langle \rho_E(0) \rangle = 1 - 2\,{\rm Re}\,[I_1(\kappa)K_1(\kappa) + I_2(\kappa)K_0(\kappa)], \tag{38}$$

where the imaginary parameter κ^2 is defined in Eq. (18). The plot of this function is shown in Fig. 5 (lower curve). Its asymptotics are

$$\langle \rho_E(0) \rangle \approx \begin{cases} \pi E/2\Delta_\xi, & E \ll \Delta_\xi, \\ 1 - \sqrt{\Delta_\xi/4E}, & E \gg \Delta_\xi. \end{cases} \tag{39}$$

[The $E \gg \Delta_\xi$ asymptotics agrees with Eq. (37) obtained by perturbative methods.]

For small $x \ll \xi$, the function $\langle \rho_E(x) \rangle$ can be obtained as a power series in x by expanding the evolution operator $e^{-2\tilde{H}t}$ in

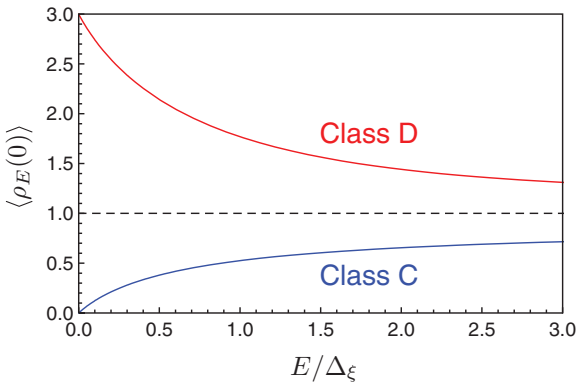

FIG. 5. (Color online) Energy dependence of the LDOS in the vicinity of the NS boundary, $\langle \rho_E^{(\infty)}(0) \rangle$, for the semi-infinite wire. The lower (upper) curve corresponds to the symmetry class C (D).

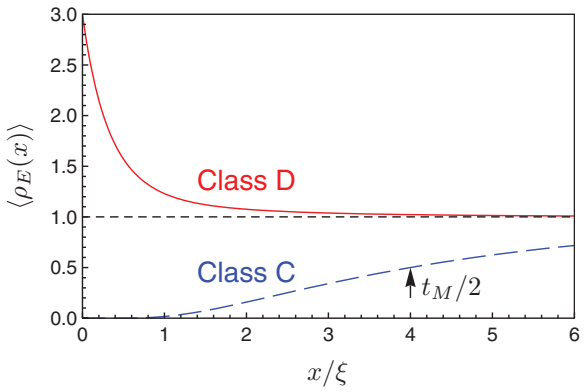

FIG. 6. (Color online) Dependence of the low-energy ($E \ll \Delta_\xi$) LDOS, $\langle \rho_E^{(\infty)}(x) \rangle$, on the distance from the SN interface for the semi-infinite wire. In the symmetry class C [lower curve, Eq. (41), sketch], LDOS depletion extends to half of the Mott scale (3), while in the symmetry class D [upper curve, Eq. (44)], excess LDOS accumulated near the interface relaxes at the localization length.

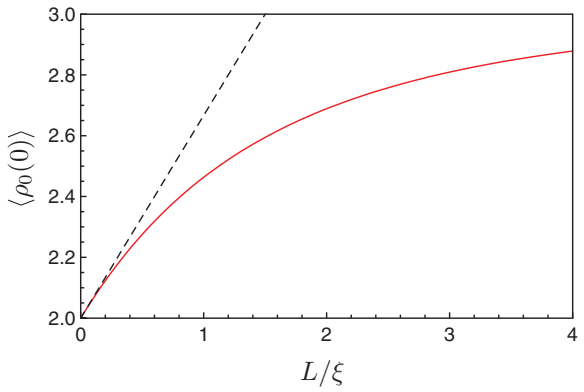

FIG. 7. (Color online) Zero-energy LDOS at the SN interface for a finite wire of length L in the symmetry class D. The dashed line shows the linear behavior for small L/ξ: $\langle \rho_0^{(L)}(0) \rangle = 2 + 2L/3\xi + \cdots$; see Eq. (33).

$t = x/\xi$ (cf. Sec. VI of Ref. 21). In the nonperturbative limit of $E \ll \Delta_\xi$, this procedure yields

$$\langle \rho_E(x) \rangle = \frac{\pi E}{2\Delta_\xi} \left(1 + 2\frac{x}{\xi} + 2\frac{x^2}{\xi^2} + \cdots \right). \tag{40}$$

According to Eq. (40), for small energies, $E \ll \Delta_\xi$, the LDOS is strongly suppressed even at the distances from the SN interface comparable to the localization length, $x \sim \xi$. In this nonperturbative regime, the LDOS depletion propagates to a much larger distance of the order of the Mott scale (3). Indeed, in the limit $E \ll \Delta_\xi$, the wave function $\Psi(Q)$ is uniformly spread over the fermionic sphere, and Eq. (25) yields $\langle \rho_E(x) \rangle = 1 - \Psi(1,1;t,s)$. To the leading approximation, Ψ at the north pole is calculated in Appendix C, and one gets (for $|t - t_M/2| \ll t_M$)

$$\langle \rho_E(x) \rangle \approx \frac{1}{2} + \frac{1}{2} \operatorname{erf} \left(\frac{t - t_M/2}{2\sqrt{t}} \right), \tag{41}$$

where $t_M = L_M/\xi$. This dependence is shown in Fig. 6 (lower curve).

2. *Symmetry class D*

Substituting the zero mode (19) into Eq. (29), one readily obtains the energy dependence of the LDOS at the SN interface for the semi-infinite wire:

$$\langle \rho_E(0) \rangle = 1 + 2\,\mathrm{Re}\,[I_1(\kappa)K_1(\kappa) + (I_0(\kappa) - 1)\,K_2(\kappa)], \tag{42}$$

with the asymptotic behavior

$$\langle \rho_E(0) \rangle \approx \begin{cases} 3 - \pi E/\Delta_\xi, & E \ll \Delta_\xi, \\ 1 + \sqrt{\Delta_\xi/4E}, & E \gg \Delta_\xi. \end{cases} \tag{43}$$

[As in class C, the $E \gg \Delta_\xi$ asymptotics agrees with the perturbative result (37).]

The function $\langle \rho_E(0) \rangle$ is shown in Fig. 5 (upper curve). Remarkably, at the lowest energies, $E \ll \Delta_\xi$, the LDOS at the SN boundary is enhanced by the factor of 3 compared to the normal case. This behavior should be contrasted with the LDOS behavior in class C, where the LDOS near the SN interface is depleted at low energies.

At zero energy, $E = 0$, the LDOS can be obtained analytically for an arbitrary relation between x, L and ξ. In the limit $\kappa \to 0$, the Hamiltonians H and $\tilde{H}$ get simplified, which allows us to evaluate the operator exponents in Eq. (13) with the help of the Lebedev-Kontorovich transformation;[36] see Appendix D. The general dependence of $\langle \rho_0(x) \rangle$ on the two parameters t and s given by Eq. (D12) is quite complicated, and we present here its limits at $t = 0$ and at $s = \infty$.

For the semi-infinite wire, the zero-energy LDOS is given by

$$\left\langle \rho_0^{(\infty)}(x) \right\rangle = 1 - \frac{\pi}{4} \frac{\partial}{\partial t} \left\{ (1 + e^{-2t}) \times \int_0^\infty k\,dk\, \frac{\sinh(\pi k/2)}{\cosh^2(\pi k/2)} e^{-(1+k^2)t/4} \right\}, \tag{44}$$

where $t = x/\xi$. The function $\rho_0^{(\infty)}(x)$ is shown in Fig. 6. Near the SN interface, the LDOS exceeds the unperturbed value by the factor of 3.

The excess LDOS accumulated near the boundary with the superconductor is relaxed to the metallic value at the scale of the localization length [whereas the LDOS depletion in the C-class case is restored at a larger Mott length scale; see Eq. (41)].

For a finite wire of length L, the zero-energy LDOS at the SN interface is given by

$$\left\langle \rho_0^{(L)}(0) \right\rangle = 3 + \frac{1}{4} \int_0^\infty k\,dk\, \tanh \frac{\pi k}{2} \times \left[\frac{k^2 - 7}{k^2 + 1} e^{-(k^2+1)s/4} - \frac{k^2 + 1}{k^2 + 9} e^{-(k^2+9)s/4} \right], \tag{45}$$

where $s = L/\xi$. This function shown in Fig. 7 interpolates between the RMT value of 2 for short wires ($L \ll \xi$) and the value of 3 in the localized regime ($L \gg \xi$). For short wires, $\langle \rho_0^{(L)}(0) \rangle = 2 + 2L/3\xi + \cdots$ (dashed line in Fig. 7) agrees with the perturbative result (33).

VI. DISCUSSION AND CONCLUSIONS

In this paper, we have solved the problem of the LDOS in a one-dimensional wire without TR symmetry connected to a

massive superconductor. Our calculation confirms qualitative expectations that the LDOS in the wire is modified in the energy window of Δ_ξ around the Fermi level within the distance of the order of ξ (up to logarithmic corrections) from the interface with the superconductor.

Propagation of superconductive correlations in the N region with the broken TR symmetry has been studied previously in the context of the Josephson coupling in a strong magnetic field.[37,38] It has been shown that while the average Josephson coupling between a pair of S islands through the N region without the TR symmetry decays exponentially, its variance decays only algebraically. This phenomenon is similar to the universal conductance fluctuations,[39,40] and originates from the diffuson-only diagram which is insensitive to the TR symmetry breaking. In the present paper we demonstrate that proximity effect without the TR symmetry manifests itself already in the average properties, provided that localization is taken into account.

The observed modification of the LDOS, in the case of a wire much longer than the localization length ξ, is totally due to localization effects and is absent in the quasiclassical description (see discussion in Sec. II). In other words, localization *enhances* proximity effect near the NS interface. Qualitatively, the effect of localization is similar to cutting the wire at the distance ξ from the interface, so that the density of states near the interface becomes similar to the RMT result in a grain of size ξ. While this similarity is only qualitative in long wires, we indeed find a true quantitative crossover to the RMT regime in the limit of short wires (much shorter than ξ). Note, however, that both in the long-wire and short-wire (RMT) limits, the number of energy levels involved in the modification of the LDOS is of order one (since $\nu\Delta_\xi\xi A \sim 1$). Thus the physics of this modification may be understood in terms of the repulsion of the lowest levels from their own mirror images (generated by the Andreev reflection), in the spirit of the superconducting ensembles in the RMT.[9]

This picture is in agreement with another important observation: the sign of the correction to the LDOS depends on the symmetry of the TR-breaking terms. There are two possible ways to break the TR symmetry: either conserving the spin symmetry (class C realizable, e.g., by an orbital magnetic field) or breaking it (class D realizable, e.g., by magnetic impurities). It is known from the RMT that corrections to the LDOS at low energies have opposite signs in these two symmetry classes (see Fig. 4). In class C, the levels repel from their own mirror images,[9] and therefore there is an effective repulsion from the Fermi level leading to a suppression of the LDOS around it. On the other hand, in class D, there is *no repulsion* of any level from its mirror image,[9] and therefore the LDOS is *enhanced* around the Fermi level (levels are "squeezed" towards it). According to the results of our calculations, the same tendency persists also for long wires, away from the RMT limit (see Figs. 5 and 6). The above argument about the repulsion of levels from their mirror images suggests that our results may be explained in terms of Mott hybridization[22] of low-lying energy levels with their Andreev-reflected images, in the spirit of our recent work.[41] We leave this interesting question for future study.

Experimentally, a modification of the LDOS by one level is usually difficult to observe (in particular, it is typically not self-averaging). However, similar effects may be of relevance in more experimentally accessible geometries (e.g., in planar NS junctions, where the corrections to the LDOS would be self-averaging due to a large area of the NS interface). Also, our calculation for the unitary symmetry class may provide helpful intuition for treating systems without TR symmetry breaking.

An important step in studying nonperturbative localization effects in such proximity systems without TR symmetry breaking was done in Ref. 42. There a scattering-matrix formalism was used to find the modification of the LDOS in TR-symmetric quantum wires close to the NS interface, in comparison with the predictions from the Usadel equations. It was found that the LDOS is reduced within the energy window of the order Δ_ξ around the Fermi level, which is qualitatively similar to our results for wires with broken TR symmetry. It would be interesting to extend the results of Ref. 42 to finite distances from the NS interface, possibly using indications from our present work. Progress in this direction may also be relevant for a theoretical analysis of experiments on Josephson junctions via Anderson insulators.[43]

Recently, a great interest has been attracted to one-dimensional hybrid structures hosting Majorana fermions at the NS boundary. Such bound zero-energy eigenstates appear if the superconductor is of a topological type.[44,45] In the random-matrix context, such systems are assigned to class B.[46–48] An evidence in favor of Majorana excitations in an InSb nanowire coupled to a superconductor has been reported in very recent experiments.[49,50] The zero-energy mode at the NS boundary is topologically protected and hence robust with respect to disorder. It is this robustness that makes the Majorana fermions promising candidates for realization of fault-tolerant quantum computations[51] and motivates further intensive research in the field.

Disorder effects on the spectral and transport characteristics of one-dimensional hybrid structures of class B models were studied both analytically and numerically within the scattering matrix formalism.[52–54] The σ-model approach developed in our paper can also be applied to the hybrid wires of class B. The characteristic distinction between classes D and B in the random-matrix approach is that the two disconnected parts of the σ-model manifold contribute with either the same (class D) or opposite (class B) signs to the partition function.[48] In our one-dimensional problem, this corresponds to the sign of the "south-pole" ($\lambda_F = -1$) contribution in Eq. (29). By changing the difference of the two wave functions in Eq. (29) into their sum, we can readily infer the LDOS in class B including the spatial profile of the Majorana mode and the depletion of the local density of other low-energy states. This calculation will be the subject of a separate forthcoming publication.[55]

ACKNOWLEDGMENTS

Hospitality of EPFL where a significant part of this work has been done is gratefully acknowledged. This work was partially supported by the Russian Ministry of Education and

Science (Contract No. 8678) (Ya.F. and M.S.) and the German Ministry of Education and Research (BMBF) (P.O. and M.S.).

APPENDIX A: σ MODEL FOR THE NS JUNCTION IN CLASSES C AND D

In this Appendix we outline the derivation of the σ model for a normal metal–superconductor junction both in the case of preserved (class C) and violated (class D) spin symmetry. The form of the σ-model action is known to be universal and depends only on the symmetries of the underlying system but not on its microscopic details. Using this fact, we will pick a particular Hamiltonian which bears all necessary symmetry properties and facilitates the derivation of the σ model.

Our strategy is as follows. We assume that the dominant disorder in the sample has the form of random potential. This potential disorder sets the elastic mean free path l, which is the shortest scale in the problem, and preserves both time-reversal and spin symmetry. This assumption allows us to consider both the superconducting and normal part of the junction on equal footing and describe them by a single σ model for a diffusive system. Then we introduce an additional relatively weak source of disorder that breaks the TR symmetry in the normal part of the junction. This is either random vector potential (class C) or magnetic impurities (class D). Violation of the TR symmetry occurs on a longer scale $L_c \gg l$. Retaining only massless degrees of freedom, we finally obtain the σ model applicable at distances longer than L_c. This will be the unitary class σ model with boundary conditions of either class C or D.

The starting point of the derivation is the Bogolyubov–de Gennes Hamiltonian. Its general form is given by Eq. (6). The Hamiltonian is a 2×2 matrix in the Nambu space. We use the notation τ for Pauli matrices acting in this space. Let us briefly discuss the structure of the Hamiltonian for our particular model. The strongest disorder is the random potential U. Singling out the corresponding term, we write the Hamiltonian as

$$\hat{\mathcal{H}}_{\mathrm{BdG}} = \hat{\mathcal{H}}_0 + \tau_z U\,. \tag{A1}$$

The most general form of the term $\hat{\mathcal{H}}_0$ is

$$\text{class C}: \quad \hat{\mathcal{H}}_0 = \tau_z\xi(\mathbf{p}) + \tau_y\Delta - \mathbf{a}\cdot\mathbf{v}, \tag{A2a}$$

$$\text{class D}: \quad \hat{\mathcal{H}}_0 = \tau_z\xi(\mathbf{p}) + \tau_y\Delta - \mathbf{b}\cdot\mathbf{s}. \tag{A2b}$$

Here we have included (i) the standard kinetic term, (ii) the superconducting order parameter Δ (assumed to be real), and (iii) the random vector potential $\mathbf{a}$ (for class C) or the random exchange field $\mathbf{b}$ due to magnetic impurities acting on electron spin (for class D). In the superconducting part of the junction, $\mathbf{a}=\mathbf{b}=0$, whereas in the normal wire, $\Delta = 0$. We proceed with the derivation of the σ model using the general form of the Bogolyubov–de Gennes Hamiltonian and will specify the effect of particular terms later.

Local density of states is expressed in terms of the retarded Green function (7). This Green function can be generated from the path integral with the action

$$S = -i\int dx\ \Phi^{+}(E+i0-\hat{\mathcal{H}}_{\mathrm{BdG}})\Phi. \tag{A3}$$

Here the vector field Φ contains both commuting and Grassmann variables and also has the structure in the Nambu space.

Bogolyubov–de Gennes Hamiltonian obeys the symmetry $\hat{\mathcal{H}} = -\tau_y\Theta\hat{\mathcal{H}}^{*}\Theta^{-1}\tau_y$ that provides the onset of specific soft modes—superconducting cooperons. In order to include these modes in the σ model, we rewrite the action (A3) in the doubled form, introducing the particle-hole structure of the fields.

$$S = -i\int dx\ \bar{\Psi}[(E+i0)\sigma_z\tau_z - \tau_z\hat{\mathcal{H}}_{\mathrm{BdG}}]\Psi, \tag{A4}$$

$$\Psi = \frac{1}{\sqrt{2}}\begin{pmatrix}\Phi\\ i\tau_y\Theta\Phi^{*}\end{pmatrix}, \quad \bar{\Psi} = \frac{1}{\sqrt{2}}(\Phi^{\dagger}\tau_z, \Phi^{T}k\tau_x\Theta^{-1}). \tag{A5}$$

We denote Pauli matrices acting in the particle-hole space by σ. Later, we will see that this space corresponds to the retarded-advanced structure in the Efetov parametrization of the unitary class σ model. The supersymmetry-breaking matrix $k = \mathrm{diag}(1,-1)_{\mathrm{FB}}$.

The matrix Θ is either unity (when spin is preserved, class C) or is_y (spin symmetry is violated, class D). In both cases, the vectors Ψ and $\bar{\Psi}$ are related by the identity $\bar{\Psi} = (C\Psi)^T$ with the charge-conjugation matrix C dependent on the symmetry class:

$$\text{class C}: \quad C = -\tau_x\begin{pmatrix} i\sigma_y & 0\\ 0 & \sigma_x\end{pmatrix}_{\mathrm{FB}}, \tag{A6a}$$

$$\text{class D}: \quad C = i\tau_x s_y\begin{pmatrix}\sigma_x & 0\\ 0 & i\sigma_y\end{pmatrix}_{\mathrm{FB}}. \tag{A6b}$$

Derivation of the σ model proceeds with averaging the statistical weight e^{-S} over potential disorder. Assuming Gaussian white-noise statistics of U, averaging yields a quartic term $\sim(\bar{\Psi}\Psi)^2$. This term is further decoupled with the help of the auxiliary matrix field $\mathcal{Q}$. The action acquires the form

$$S = \int dx\left[\frac{\pi\nu_0}{8\tau}\,\mathrm{str}\,\mathcal{Q}^2 - i\bar{\Psi}\left(E\sigma_z\tau_z + \frac{i\mathcal{Q}}{2\tau} - \tau_z\hat{\mathcal{H}}_0\right)\Psi\right]. \tag{A7}$$

Here $\hat{\mathcal{H}}_0$ is defined in Eqs. (A1) and (A2), and ν_0 is the density of states per one spin projection. The field $\mathcal{Q}$ is normalized such that the infinitesimal imaginary part $i0\sigma_z\tau_z$ is replaced by $i\mathcal{Q}/2\tau$ where τ is the disorder-induced mean free time.

Next, we integrate out the vector field Ψ and perform the saddle-point analysis of the resulting action

$$S = \frac{\pi\nu_0}{8\tau}\int dx\,\mathrm{str}\,\mathcal{Q}^2 - \frac{1}{2}\,\mathrm{str}\ln\left(E\sigma_z\tau_z + \frac{i\mathcal{Q}}{2\tau} - \tau_z\hat{\mathcal{H}}_0\right). \tag{A8}$$

The term proportional to E as well as all the terms in $\hat{\mathcal{H}}_0$ other than the kinetic term [see Eq. (A2)] are relatively small. We first consider saddle points of the action (A8) with $E=0$ and $\hat{\mathcal{H}}_0 = \tau_z\xi(\mathbf{p})$. There is always one saddle point equivalent to the self-consistent Born approximation for the average Green function. It corresponds to replacing $i0$ in the original action with $i/2\tau$; hence $\mathcal{Q} = \sigma_z\tau_z$ is a legitimate saddle point. We can generate other saddle points with the help of the global gauge symmetry of the fermionic action (A7). Indeed, let us change the variables in Eq. (A7): $\Psi \mapsto U\Psi$, $\bar{\Psi}\mapsto\bar{\Psi}\bar{U}$ with some matrix U obeying the relation $\bar{U}U = 1$. (Charge conjugation

for matrices is defined as $\bar{U} = CU^TC^T$.) This transformation cannot alter the value of the action for $\mathcal{Q}$. At the same time, U commutes with $\xi(\mathbf{p})$ since U is constant in space. Hence the rotation of Ψ can be compensated by $\mathcal{Q} \mapsto U\mathcal{Q}U^{-1}$. This allows us to generate the whole saddle manifold of the σ model,

$$\mathcal{Q} = U\sigma_z\tau_z\bar{U}. \tag{A9}$$

The manifold is characterized by the conditions $\mathcal{Q}^2 = 1$ and $\mathcal{Q} = \bar{\mathcal{Q}} = C\mathcal{Q}^TC^T$ (this space of Q matrices corresponds to disordered systems of the symmetry class AI, in the classification of Zirnbauer[32,56]).

The σ-model action is the result of the expansion of Eq. (A8) to the first order in scalars Δ and E and to the second order in vectors ∇Q, $\mathbf{a}$, and $\mathbf{b}$. Assuming $\mathbf{a}$ and $\mathbf{b}$ are Gaussian white-noise random quantities, we obtain

$$S = \frac{\pi\nu_0}{8}\int dx\,\mathrm{str}\{D\big(\nabla\mathcal{Q}\big)^2 + 4i\big(E\sigma_z\tau_z + i\tau_x\Delta\big)\mathcal{Q} + L_{\mathrm{sb}}\}, \tag{A10}$$

with the symmetry-breaking term

$$\text{class C}: \quad L_{\mathrm{sb}} = -D\langle\mathbf{a}\rangle^2[\tau_z,\mathcal{Q}]^2, \tag{A11a}$$

$$\text{class D}: \quad L_{\mathrm{sb}} = -\frac{\tau}{3}\langle\mathbf{b}\rangle^2[\tau_z\mathbf{s},\mathcal{Q}]^2. \tag{A11b}$$

The above action contains simultaneously all possible terms of our σ model. Now we analyze the theory in particular cases keeping only the relevant terms in Eq. (A10). Let us start with the superconducting part of the junction. Assuming a bulk superconductor with large density of states and diffusion constant, we keep only E and Δ terms and neglect fluctuations of $\mathcal{Q}$. This allows us to fix $\mathcal{Q} = \mathcal{Q}_S$ at the saddle point of the σ-model action,

$$\mathcal{Q}_S = \begin{pmatrix} \sigma_z\cos\theta_S & \sin\theta_S \\ \sin\theta_S & -\sigma_z\cos\theta_S \end{pmatrix}_{\mathrm{N}}, \quad \tan\theta_S = \frac{i\Delta}{E}. \tag{A12}$$

Now consider the normal part of the junction first with preserved spin symmetry (class C). Here $\Delta = 0$ while random magnetic field, $\langle\mathbf{a}\rangle^2 \neq 0$, has a strong effect violating the TR symmetry. This leads to the additional constraint $[\tau_z,\mathcal{Q}] = 0$ making the matrix $\mathcal{Q}$ diagonal in the Nambu space. The condition $\mathcal{Q} = \bar{\mathcal{Q}}$ with C from Eq. (A6a) leads to the representation

$$\mathcal{Q} = \begin{pmatrix} Q & 0 \\ 0 & \Xi Q^T\Xi^T \end{pmatrix}_{\mathrm{N}}, \tag{A13}$$

where Ξ is the matrix defined in Eq. (12a). In the normal part of the junction, the σ model action (A10) can be written in terms of Q with the only constraint $Q^2 = 1$. Then one obtains exactly the action (10) (with $\nu = \nu_0$) for the unitary class σ model, with the particle-hole structure playing the role of the retarded-advanced space.

Let us now consider the case of broken spin symmetry (class D). The matrix $\mathcal{Q}$ has a structure in the additional spin space and obeys the relation $\mathcal{Q} = \bar{\mathcal{Q}}$ with C from Eq. (A6b). Taking into account random exchange field, $\langle\mathbf{b}\rangle^2 \neq 0$, we get the constraint $[\tau_z\mathbf{s},\mathcal{Q}] = 0$. It makes $\mathcal{Q}$ diagonal in the Nambu space and trivial (unit matrix) in the spin space. The representation (A13) again applies but now with Ξ from Eq. (12b). In terms of Q, the σ model action is again given by Eq. (10). The trace over the spin space doubles the density of states in the prefactor of the action: $\nu = 2\nu_0$.

The last ingredient of the theory is the boundary term (11). In terms of the matrix $\mathcal{Q}$, boundary action is known to be[18]

$$S_\Gamma = -\frac{1}{2}\sum_i \mathrm{str}\ln(1 + e^{-2\beta_i}\mathcal{Q}_S\mathcal{Q}). \tag{A14}$$

Using Eqs. (A12) and (A13), we trace the Nambu (and optionally spin) space and obtain the boundary action in the form

$$S_\Gamma = -\frac{1}{2}\sum_i \mathrm{str}\ln[1 + e^{-2\beta_i}\cos\theta_S(Q\sigma_z - \sigma_z\Xi Q^T\Xi^T) - e^{-4\beta_i}Q\Xi Q^T\Xi^T]. \tag{A15}$$

If the gap in the superconductor Δ is sufficiently large, we may neglect $\cos\theta_S$ in Eq. (A15) and obtain the simplified boundary action (11). An accurate estimate for this approximation gives the condition $\sum_i \mathcal{T}_i^{1/2}E \ll \Delta$ in class C and $\sum_i \mathcal{T}_i^{1/2}\tilde{\lambda}_B E \ll \Delta$ in class D, where $\mathcal{T}_i$ are Andreev transmission coefficients given by Eq. (23) and $\tilde{\lambda}_B$ is the characteristic scale of λ_B involved. Up to a factor of order 2, we may estimate $\sum_i \mathcal{T}_i^{1/2} \sim \sum_i T_i = g_N$, the normal conductance of the SN interface. We also estimate $\tilde{\lambda}_B \sim \max(\delta,\Delta_\xi)/E$, where δ is the mean level spacing in the N part, as defined in Eq. (32). As a result, we find the applicability conditions for the boundary term (11):

$$\Delta \gg \begin{cases} g_N E & \text{in class C,} \\ g_N\max(\delta,\Delta_\xi) & \text{in class D.} \end{cases} \tag{A16}$$

APPENDIX B: DERIVATION OF THE LDOS EXPRESSIONS (21) AND (27)

1. Efetov's parametrization

We adopt the standard Efetov's parametrization[18] of the 4×4 matrix Q for the unitary symmetry class:

$$Q = U_\eta^{-1}Q_0U_\eta, \tag{B1}$$

where the FB-diagonal central part, Q_0, contains only commuting variables:

$$Q_0 = \begin{pmatrix} Q_0^{\mathrm{FF}} & 0 \\ 0 & Q_0^{\mathrm{BB}} \end{pmatrix}_{\mathrm{FB}}, \tag{B2a}$$

$$Q_0^{\mathrm{FF}} = \begin{pmatrix} \lambda_F & e^{i\varphi_F}\sqrt{1-\lambda_F^2} \\ e^{-i\varphi_F}\sqrt{1-\lambda_F^2} & -\lambda_F \end{pmatrix}_{\mathrm{RA}}, \tag{B2b}$$

$$Q_0^{\mathrm{BB}} = \begin{pmatrix} \lambda_B & ie^{i\varphi_B}\sqrt{\lambda_B^2-1} \\ ie^{-i\varphi_B}\sqrt{\lambda_B^2-1} & -\lambda_B \end{pmatrix}_{\mathrm{RA}}, \tag{B2c}$$

while Grassmann variables reside in the RA-diagonal matrix

$$U_\eta = \begin{pmatrix} u & 0 \\ 0 & v \end{pmatrix}_{\mathrm{RA}}, \tag{B3a}$$

$$u = \exp\begin{pmatrix} 0 & \sigma \\ \sigma^* & 0 \end{pmatrix}_{\mathrm{FB}}, \quad v = \exp\begin{pmatrix} 0 & \rho \\ \rho^* & 0 \end{pmatrix}_{\mathrm{FB}}. \tag{B3b}$$

Integration variables change in the intervals $\lambda_F \in [-1,1]$, $\lambda_B \in [1,\infty)$, and $\varphi_{F,B} \in [0,2\pi)$, with the invariant

measure

$$dQ = \frac{d\lambda_B d\lambda_F}{(\lambda_B-\lambda_F)^2}\frac{d\varphi_B d\varphi_F}{(2\pi)^2}\, d\rho^* d\rho\, d\sigma^* d\sigma\,. \tag{B4}$$

2. Boundary term

Substituting Eqs. (4) and (B2) into the boundary action (11), after some algebra we obtain for the class C [Ξ is given by Eq. (12a)]

$$S_\Gamma = \left[1 - \frac{\lambda_B-\lambda_F}{2}(\sigma-\rho^*)(\sigma^*+\rho)\frac{\partial}{\partial\lambda_B}\right] S_0^{\mathrm{C}}(\lambda_B), \tag{B5}$$

where the action $S_0^{\mathrm{C}}(\lambda_B)$ is given by Eq. (22).

For class D [Ξ is given by Eq. (12b)] we get a similar result:

$$S_\Gamma = \left[1 - \frac{\lambda_B-\lambda_F}{2}(\sigma-\rho^*)(\sigma^*+\rho)\frac{\partial}{\partial\lambda_F}\right] S_0^{\mathrm{D}}(\lambda_F), \tag{B6}$$

where the action $S_0^{\mathrm{D}}(\lambda_F)$ is given by Eq. (28).

3. Expression for the LDOS in terms of the effective quantum mechanics

In the language of the effective quantum mechanics,[27] with the coordinate along the wire playing the role of imaginary time, calculation of the functional integral (9) for $\langle\rho_E(x)\rangle$ is performed in two steps. First we evaluate the functional integral along the segment $[x,L]$ of the wire, which generates the "singlet" wave function

$$\Psi(Q(x);s) = e^{-2Hs}\circ 1, \tag{B7}$$

where $s=(L-x)/\xi$ is the dimensionless distance from the open end. By symmetry, the "radial" wave function $\Psi(Q(x);s)$ depends only on the variables λ_F and λ_B.

At the point x, the LDOS preexponent $\mathrm{str}(k\Lambda Q(x))$ introduces the multiplet of states $Q\Psi(Q)$. Then, evaluation of the functional integral at the segment $[0,x]$ amounts to following the evolution of the multiplet $P\equiv Q\Psi(Q)$ from the observation point x down to the SN interface. The resulting matrix P is known[18,27] to be of the form (B2) with the elements modified according to

$$\lambda_F \to g_F\lambda_F, \quad \sqrt{1-\lambda_F^2}\to f_F\sqrt{1-\lambda_F^2}, \tag{B8a}$$

$$\lambda_B \to g_B\lambda_B, \quad \sqrt{\lambda_B^2-1}\to f_B\sqrt{\lambda_B^2-1}. \tag{B8b}$$

The evolution equations for the functions f_F and f_B which determine the density-density response function (RA-off-diagonal components) have been derived in Ref. 27. For the LDOS, we need the RA-diagonal components, g_F and g_B, whose evolution is described by the coupled differential equations

$$\frac{1}{2}\frac{\partial g_F}{\partial t} = -Hg_F + \frac{1-\lambda_F^2}{\lambda_F}\frac{\partial g_F}{\partial\lambda_F} + \frac{\lambda_B}{\lambda_F}M\Delta g, \tag{B9a}$$

$$\frac{1}{2}\frac{\partial g_B}{\partial t} = -Hg_B + \frac{\lambda_B^2-1}{\lambda_B}\frac{\partial g_B}{\partial\lambda_B} + \frac{\lambda_F}{\lambda_B}M\Delta g, \tag{B9b}$$

where t is the distance from the point x measured in units of ξ, $\Delta g = g_B - g_F$, and

$$M = \frac{\lambda_F\lambda_B - 1}{(\lambda_B-\lambda_F)^2}. \tag{B10}$$

The initial conditions for the evolution (B9) are $g_F = g_B = \Psi(Q(x);s)$ at $t=0$.

Calculation of the functional integral (9) along the segment $[0,x]$ is equivalent to solving Eqs. (B9) up to $t=x/\xi$. As a result, one ends up with a single integral over $\mathcal{Q}\equiv Q(0)$ at the SN interface:

$$\langle\rho_E(x)\rangle = \mathrm{Re}\int d\mathcal{Q}\,\frac{\mathrm{str}(k\Lambda P(\mathcal{Q};t,s))}{4}\, e^{-S_\Gamma[\mathcal{Q}]}. \tag{B11}$$

Using Eqs. (B2) and (B8), we express

$$\frac{\mathrm{str}(k\Lambda P)}{4} = \Phi_+ - (\sigma\sigma^*+\rho\rho^*)\Phi_- \tag{B12}$$

in terms of two functions:

$$\Phi_\pm = \frac{g_B\lambda_B \pm g_F\lambda_F}{2}. \tag{B13}$$

Combining Eqs. (B9a) and (B9b) one immediately obtains[20] that the function Φ_- exhibits a simple evolution with the Hamiltonian (15):

$$\frac{\partial\Phi_-}{\partial t} = -2H\Phi_-. \tag{B14}$$

Taking into account the boundary condition $\Phi_- = (\lambda_B-\lambda_F)\Psi(Q(x),s)$ at $t=0$ and the definition (16) of the Hamiltonian $\tilde{H}$, one arrives at

$$\Phi_-(\mathcal{Q};t,s) = (\lambda_B-\lambda_F)\Psi(\lambda_F,\lambda_B;t,s), \tag{B15}$$

where

$$\Psi(\lambda_F,\lambda_B;t,s) = e^{-2\tilde{H}t}\Psi(Q(x),s). \tag{B16}$$

Evolution of the function $\Phi_+(\mathcal{Q};t,s)$ is more complicated and can be in principle deduced from Eqs. (B9).

Evaluating the integral (B11) using Eqs. (B4), (B5), and (B12), we get the LDOS for the symmetry class C:

$$\langle\rho_E(x)\rangle = \mathrm{Re}\,\Phi_+(1,1;t,s) + \frac{1}{2}\mathrm{Re}\int_{-1}^{1}d\lambda_F\int_1^\infty d\lambda_B \times\frac{\partial e^{-S_0(\lambda_B)}}{\partial\lambda_B}\Psi(\lambda_F,\lambda_B;t,s), \tag{B17}$$

where the first term comes from the anomaly associated with the singularity of the measure (B4) at the origin.[18] Though the general evolution of Φ_+ described by Eqs. (B9) is quite complicated, its value at the origin, $\Phi_+(\Lambda)$, can be readily found. Indeed, in the absence of coupling to the superconductor ($T_i=0$), one should reproduce the normal-state result, $\langle Q\rangle = \Lambda$. Hence $\Phi_+(1,1;t,s)=1$, leading to Eq. (21) .

Similar calculations for the symmetry class D [with Eq. (B6) instead of (B5)] lead to Eq. (27) .

APPENDIX C: EVOLUTION AT THE MOTT SCALE: DIFFUSION AND DRIFT

In this Appendix, we approximately calculate the wave function $\Psi(\lambda_F,\lambda_B;t,s)$ defined in Eq. (19) for $t\gg 1$ and $|\kappa|^2\ll 1$. First consider the wave function

$$\Psi(\lambda_F,\lambda_B;0,s) = e^{-2Hs}\circ 1. \tag{C1}$$

It interpolates between $\Psi(\lambda_F,\lambda_B) \equiv 1$ at $s = 0$ and $\Psi_0(\lambda_F,\lambda_B)$ given by Eq. (19) at $s \to \infty$. We will use the following properties of the wave function (C1).

(1) It does not develop any singularity at $\lambda_B \in [1;\infty)$ and $\lambda_F \in [-1;1]$.

(2) It varies at the length scale $\lambda \sim |\kappa|^{-2} \gg 1$ in both λ_F and λ_B. In particular, the dependence on λ_F is very weak.

(3) It is universally normalized at the origin: $\Psi(1,1;0,s) \equiv 1$. This follows from the supersymmetry [there is a zero mode of H with $\Psi(1,1) = 1$, and all the excited modes have $\Psi(1,1) = 0$].

Then we note that the fermionic part $\tilde{H}_F$ of the Hamiltonian (16) has a discrete spectrum with a level spacing of order one, and therefore, at $t \gg 1$, only the lowest eigenstate of $\tilde{H}_F$ survives. By the perturbation theory, its energy is of the order $|\kappa|^4$, and, since we will be interested at the logarithmic scales $t \sim \ln|\kappa|^{-2}$, it can be neglected, as well as its λ_F dependence. Therefore, at $t \gg 1$, we can approximate

$$\Psi(\lambda_F,\lambda_B;t,s) \approx e^{-2\tilde{H}_B t}\Psi(1,\lambda_B;0,s). \tag{C2}$$

To understand the evolution in λ_B, it is convenient to change to the logarithmic coordinate θ_B defined by

$$\lambda_B = \cosh\theta_B. \tag{C3}$$

In this variable, $\Psi(1,\theta_B;0,s) \approx 1$ for $\theta \lesssim \ln|\kappa|^{-2}$ (or even at larger θ_B, for small s). In terms of θ_B, the bosonic Hamiltonian takes the form

$$\tilde{H}_B = -\frac{1}{2}\frac{\partial^2}{\partial\theta_B^2} - \frac{1}{2}\coth\theta_B\frac{\partial}{\partial\theta_B} + \frac{\kappa^2}{16}\cosh\theta_B. \tag{C4}$$

This Hamiltonian consists of three terms. The first term describes a diffusion in θ_B. The second term produces a drift towards the origin $\theta_B = 0$. Note that the velocity of this drift equals $1/2$ at $\theta_B \gg 1$ and differs from $1/2$ only near the origin (in such a way that the total drift time changes by a small correction of order one). The third, potential, term of the Hamiltonian is relevant at $\theta_B \gtrsim \theta_M/2$, where we define the Mott scale

$$\theta_M = 2\ln(|\kappa|^{-2}) \approx L_M/\xi. \tag{C5}$$

[We have introduced the coefficient 2 in the above definition in order to relate θ_M to the conventional definition (3) of the Mott length scale L_M]. The third term suppresses the wave function at $\theta_B > \theta_M/2$ for $t \gtrsim 1$, regardless of the initial wave function (C1). Therefore, at $t \sim 1$, the wave function $\Psi(\lambda_F,\lambda_B;t,s)$ may be approximated as a step function

$$\Psi(\theta_B) \approx \theta(\theta_M/2 - \theta_B), \tag{C6}$$

independently of λ_F and s. Note that the width of this step function is of order one (in the units of θ_B), but, at our level of precision, we are not interested in details at such a short length scale.

Finally, we may approximately calculate the result of the evolution (C2) by applying the first two terms of the Hamiltonian (C4) to the step function (C6). At our level of precision, we may also neglect the difference of the drift velocity from $1/2$. We thus find the following result:

$$\Psi(\lambda_F,\lambda_B;t,s) \approx \frac{1}{2}\left[1 - \mathrm{erf}\left(\frac{\theta_B - \theta_M/2 + t}{2\sqrt{t}}\right)\right], \tag{C7}$$

where θ_B is related to λ_B by Eq. (C3).

In particular, at $\lambda_B = 1$, we find

$$\Psi(\lambda_F,1;t,s) \approx \frac{1}{2}\left[1 - \mathrm{erf}\left(\frac{t - \theta_M/2}{2\sqrt{t}}\right)\right]. \tag{C8}$$

Note that the location of this erf function is at $L_M/2$, which is two times closer than the similar "erf" feature in the correlation function of the local density of states in the wire.[21,57]

The result (C8) describes the crossover of $\Psi(\lambda_F,1;t,s)$ from one to zero around $t \approx \theta_M/2$ and is valid only in the vicinity of this point. To estimate the range of validity of our approximations, we recall that we neglected the details of the evolution of the initial state at $t \lesssim 1$. This effectively introduces an uncertainty $\Delta t \sim 1$ in the final result (C8). Its range of validity may be therefore estimated from its insensitivity to this uncertainty, which leads to the condition $|t - \theta_M/2| \ll \theta_M$ (note that this range of validity is larger than the width of the crossover itself).

APPENDIX D: DENSITY OF STATES AT $E = 0$ FOR CLASS D

The LDOS in class D can be calculated exactly for quasiparticles right at the Fermi energy ($E \to 0$). In this limit, the "fermionic" variable $q \in [0,\kappa]$ defined in Eq. (20) is small, and the wave function (13) can be expanded as

$$\Psi(p,q;t,s) = \psi_0(p;t,s) + q^2\psi_1(p;t,s) + o(q^2). \tag{D1}$$

Substituting this series into the general expression (29) we see that the smallness of $\Psi(1,\lambda_B;t,s) - \Psi(-1,\lambda_B;t,s) \propto \kappa^2$ is compensated by the large value of the integral over λ_B, leading to a finite limit at $\kappa \to 0$:

$$\langle\rho_0(x)\rangle = 1 + 2\int_0^\infty \psi_1(p;t,s)p\,dp. \tag{D2}$$

The function $\Psi(p,q;t,s)$ is obtained through the Hamiltonian evolution (13). Since the Hamiltonians H and $\tilde{H}$ are related by the transformation (16), it suffices to study only the $\tilde{H}$ evolution. In the order q^2, the fermionic part (17b) of the Hamiltonian $\tilde{H}$ acts as follows (at $\kappa = 0$):

$$\tilde{H}_F\begin{pmatrix}1\\ q^2\end{pmatrix} = \begin{pmatrix}-q^2/8\\ q^2\end{pmatrix} + o(q^2),$$

and one immediately obtains the evolution of an arbitrary function $\chi(p,q) = \chi_0(p) + q^2\chi_1(p) + o(q^2)$ by the Hamiltonian $\tilde{H}$ to the desired accuracy:

$$e^{-2\tilde{H}t}\chi(p,q) = \left(1 + q^2\frac{1 - e^{-2t}}{8}\right)\hat{U}_t\chi_0(p) + q^2e^{-2t}\hat{U}_t\chi_1(p) + o(q^2). \tag{D3}$$

Here

$$\hat{U}_t = e^{-2\tilde{H}_B^0 t} \tag{D4}$$

is the evolution operator for the bosonic Hamiltonian (17a) in the limit $\kappa = 0$:[21]

$$\tilde{H}_B^0 = \frac{1}{8}\left(-\frac{1}{p}\frac{\partial}{\partial p}p^3\frac{\partial}{\partial p} + p^2\right). \tag{D5}$$

This Hamiltonian defined at the semiaxis $p > 0$ has a continuous spectrum $E_k = (k^2+1)/8$ with the eigenfunctions $K_{ik}(p)/p$.

The general expression (13) for $\Psi(p,q;t,s)$ can be identically rewritten in the form

$$\Psi(p,q;t,s) = e^{-2\hat{H}t}\Psi_0(p,q) + e^{-2\hat{H}t}(p^2-q^2) \times e^{-2\hat{H}s}\frac{1-\Psi_0(p,q)}{p^2-q^2}, \quad \text{(D6)}$$

where we used the relation (16) and extracted the zero mode of H. Now expanding in q^2 and successively applying Eq. (D3), we arrive at

$$\psi_1(p;t,\infty) = \frac{1-e^{-2t}}{8}\hat{U}_t\Psi_0(p) + e^{-2t}\hat{U}_t\Pi_0(p), \quad \text{(D7)}$$

$$\psi_1(p;t,s) = \psi_1(p;t,\infty) + \frac{1-e^{-2(t+s)}}{8}\hat{U}_t p^2\hat{U}_s Y(p) + e^{-2(t+s)}\hat{U}_t p^2\hat{U}_s Z(p) - e^{-2t}\hat{U}_{t+s}Y(p), \quad \text{(D8)}$$

where

$$\Psi_0(p) = \Psi_0(p,0), \quad \Pi_0(p) = \partial_{q^2}\Psi_0(p,q)\big|_{q=0},$$

$$Y(p) = \frac{1-\Psi_0(p)}{p^2}, \quad Z(p) = \frac{Y(p)-\Pi_0(p)}{p^2}.$$

The evolution operator U_t becomes trivial in the basis of the eigenfunctions of the Hamiltonian (D5), where it amounts to multiplication by $e^{-(k^2+1)t/4}$. Transition to the basis of $K_{ik}(p)/p$ is known as the Lebedev-Kontorovich transformation.[36] For the zero mode $\Psi_0(p,q)$ given by Eq. (19), we obtain

$$\Psi_0(p) = \int_0^\infty k\,dk\,\frac{k^2+1}{2}\tanh\frac{\pi k}{2}\frac{K_{ik}(p)}{p}, \quad \text{(D9a)}$$

$$\Pi_0(p) = \int_0^\infty k\,dk\,\frac{k^2+5}{8}\tanh\frac{\pi k}{2}\frac{K_{ik}(p)}{p}, \quad \text{(D9b)}$$

$$Y(p) = \frac{2}{\pi}\int_0^\infty \frac{k\,dk}{k^2+1}\sinh\frac{\pi k}{2}\frac{K_{ik}(p)}{p}, \quad \text{(D9c)}$$

$$Z(p) = \frac{2}{\pi}\int_0^\infty \frac{k\,dk}{(k^2+1)(k^2+9)}\sinh\frac{\pi k}{2}\frac{K_{ik}(p)}{p}. \quad \text{(D9d)}$$

In order to evaluate the action of the composite operator $\hat{U}_t p^2\hat{U}_s$ in Eq. (D8) one has to reexpand $pK_{ik}(p)$ in the eigenfunctions of the Hamiltonian (D5) which is performed with the help of the Lebedev-Kontorovich transformation:

$$pK_{ik}(p) = \frac{1}{2}\int_0^\infty l\,dl\,\frac{(l^2-k^2)\sinh\pi l}{\cosh\pi l-\cosh\pi k}\frac{K_{il}(p)}{p}. \quad \text{(D10)}$$

Substituting Eqs. (D9a) and (D9b) into Eqs. (D2) and (D7), and integrating over p with the help of

$$\int_0^\infty K_{ik}(p)dp = \frac{\pi}{2\cosh\pi k/2}, \quad \text{(D11)}$$

we obtain the result (44) for the LDOS in the infinite wire, $\langle\rho_0^{(\infty)}(x)\rangle$.

The general expression for the zero-energy LDOS in a finite wire can be written with the help of Eqs. (D2), (D8), (D9c), (D9d), and (D10) as

$$\langle\rho_0(x)\rangle = \langle\rho_0^{(\infty)}(x)\rangle - 2e^{-2t}\int_0^\infty \frac{k\,dk}{k^2+1}\tanh\frac{\pi k}{2}e^{-(k^2+1)(t+s)/4} + \frac{1}{4}\int_0^\infty\int_0^\infty \frac{k\,dk\,l\,dl(k^2-l^2)}{\cosh\pi k-\cosh\pi l}\sinh\frac{\pi k}{2}\sinh\frac{\pi l}{2} \times\left[\frac{1}{k^2+1}-\frac{e^{-2(t+s)}}{k^2+9}\right]e^{-(k^2+1)s/4-(l^2+1)t/4}. \quad \text{(D12)}$$

[1] G. Deutscher and P. G. de Gennes, in *Superconductivity*, edited by R. D. Parks (Dekker, New York, 1969), pp. 1005–1034.

[2] A. F. Andreev, Zh. Eksp. Teor. Fiz. **46**, 1823 (1964) [Sov. Phys. JETP **19**, 1228 (1964)].

[3] A. D. Zaikin and G. F. Zharkov, Fiz. Nizk. Temp. **7**, 375 (1981) [Sov. J. Low Temp. Phys. **7**, 184 (1981)].

[4] W. Belzig, C. Bruder, and G. Schön, Phys. Rev. B **54**, 9443 (1996).

[5] A. A. Golubov, M. Yu. Kupriyanov, and E. Il'ichev, Rev. Mod. Phys. **76**, 411 (2004).

[6] D. Taras-Semchuk and A. Altland, Phys. Rev. B **64**, 014512 (2001).

[7] Trajectory randomization is assumed to be fast. The opposite case is considered in Ref. 6.

[8] F. Zhou, P. Charlat, B. Spivak, and B. Pannetier, J. Low Temp. Phys. **110**, 841 (1998); D. A. Ivanov, R. von Roten, and G. Blatter, Phys. Rev. B **66**, 052507 (2002).

[9] A. Altland and M. R. Zirnbauer, Phys. Rev. B **55**, 1142 (1997).

[10] A. Altland, B. D. Simons, and D. Taras-Semchuk, Adv. Phys. **49**, 321 (2000).

[11] R. Gade and F. Wegner, Nucl. Phys. B **360**, 213 (1991).

[12] A. A. Nersesyan, A. M. Tsvelik, and F. Wenger, Phys. Rev. Lett. **72**, 2628 (1994); Nucl. Phys. B **438**, 561 (1995).

[13] T. Senthil, M. P. A. Fisher, L. Balents, and C. Nayak, Phys. Rev. Lett. **81**, 4704 (1998).

[14] A. Altland, B. D. Simons, and M. R. Zirnbauer, Phys. Rep. **359**, 283 (2002).

[15] P. W. Anderson, Phys. Rev. **109**, 1492 (1958).

[16] The same energy scale can be expressed as $\Delta_\xi \sim (\nu A\xi)^{-1}$, where ν is the bulk density of states and A is the wire cross section. The two expressions agree up to a numerical coefficient, due to the relation (5) for the localization length.

[17] K. B. Efetov, Adv. Phys. **32**, 53 (1983).

[18] K. B. Efetov, *Supersymmetry in Disorder and Chaos* (Cambridge University Press, New York, 1997).

[19] M. A. Skvortsov and P. M. Ostrovsky, Pis'ma Zh. Eksp. Teor. Fiz. **85**, 79 (2007) [JETP Lett. **85**, 72 (2007)].

[20] D. A. Ivanov and M. A. Skvortsov, J. Phys. A: Math. Theor. **41**, 215003 (2008).

[21] D. A. Ivanov, P. M. Ostrovsky, and M. A. Skvortsov, Phys. Rev. B **79**, 205108 (2009).

[22] N. F. Mott, Philos. Mag. **17**, 1259 (1968); **22**, 7 (1970).

[23] K. Usadel, Phys. Rev. Lett. **25**, 507 (1970).

[24]A. Altland and B. D. Simons, *Condensed Matter Field Theory*, 2nd ed. (Cambridge University Press, Cambridge, UK, 2010).
[25]M. A. Skvortsov, A. I. Larkin, and M. V. Feigel'man, Phys. Rev. B **63**, 134507 (2001).
[26]O. N. Dorokhov, Pis'ma Zh. Eksp. Teor. Fiz. **36**, 259 (1982) [Sov. Phys. JETP Lett. **36**, 318 (1982)].
[27]K. B. Efetov and A. I. Larkin, Zh. Eksp. Teor. Fiz. **85**, 764 (1983) [Sov. Phys. JETP **58**, 444 (1983)].
[28]M. A. Skvortsov, V. E. Kravtsov, and M. V. Feigel'man, Pis'ma Zh. Eksp. Teor. Fiz. **68**, 78 (1998) [JETP Lett. **68**, 84 (1998)].
[29]A. Altland, B. D. Simons, and D. Taras-Semchuk, Pis'ma Zh. Eksp. Teor. Fiz. **67**, 21 (1998) [JETP Lett. **67**, 22 (1998)].
[30]R. Bundschuh, C. Cassanello, D. Serban, and M. R. Zirnbauer, Phys. Rev. B **59**, 4382 (1999).
[31]P. M. Ostrovsky, M. A. Skvortsov, and M. V. Feigel'man, Phys. Rev. Lett. **87**, 027002 (2001).
[32]V. A. Koziy and M. A. Skvortsov, Pis'ma Zh. Eksp. Teor. Fiz. **94**, 240 (2011) [JETP Lett. **94**, 222 (2011)].
[33]For moderate symmetry breaking, crossover between symmetry classes has been studied in Ref. 32.
[34]C. W. J. Beenakker, Phys. Rev. B **46**, 12841 (1992).
[35]A. V. Andreev and B. L. Altshuler, Phys. Rev. Lett. **75**, 902 (1995).
[36]A. Erdelyi, W. Magnus, and F. Oberhettinger, *Tables of Integral Transforms*, Vol. 2 (McGraw-Hill, New York, 1954).
[37]B. Spivak and F. Zhou, Phys. Rev. Lett. **74**, 2800 (1995).
[38]V. M. Galitski and A. I. Larkin, Phys. Rev. Lett. **87**, 087001 (2001).
[39]B. L. Altshuler, Pis'ma Zh. Eksp. Teor. Fiz. **41**, 530 (1985) [Sov. Phys. JETP Lett. **41**, 648 (1985)].
[40]P. A. Lee and A. D. Stone, Phys. Rev. Lett. **55**, 1622 (1985).
[41]D. A. Ivanov, M. A. Skvortsov, P. M. Ostrovsky, and Ya. V. Fominov, Phys. Rev. B **85**, 035109 (2012).
[42]M. Titov and H. Schomerus, Phys. Rev. B **67**, 024410 (2003).
[43]A. Frydman and Z. Ovadyahu, Europhys. Lett. **33**, 217 (1996); Phys. Rev. B **55**, 9047 (1997).
[44]Y. Oreg, G. Refael, and F. von Oppen, Phys. Rev. Lett. **105**, 177002 (2010).
[45]R. M. Lutchyn, J. D. Sau, and S. Das Sarma, Phys. Rev. Lett. **105**, 077001 (2010).
[46]M. Caselle, arXiv:cond-mat/9610017.
[47]M. Bocquet, D. Serban, and M. R. Zirnbauer, Nucl. Phys. B **578**, 628 (2000).
[48]D. A. Ivanov, J. Math. Phys. **43**, 126 (2002).
[49]V. Mourik, K. Zuo, S. M. Frolov, S. R. Plissard, E. P. A. M. Bakkers, and L. P. Kouwenhoven, Science **336**, 1003 (2012).
[50]M. T. Deng, C. L. Yu, G. Y. Huang, M. Larsson, P. Caroff, and H. Q. Xu, Nano Lett. **12**, 6414 (2012).
[51]C. W. J. Beenakker, arXiv:1112.1950, and references therein.
[52]P. W. Brouwer, M. Duckheim, A. Romito, and F. von Oppen, Phys. Rev. Lett. **107**, 196804 (2011); Phys. Rev. B **84**, 144526 (2011).
[53]F. Pientka, G. Kells, A. Romito, P. W. Brouwer, and F. von Oppen, Phys. Rev. Lett. **109**, 227006 (2012).
[54]D. I. Pikulin, J. P. Dahlhaus, M. Wimmer, H. Schomerus, and C. W. J. Beenakker, New J. Phys. **14**, 125011 (2012).
[55]D. A. Ivanov, P. M. Ostrovsky, and M. A. Skvortsov (in preparation).
[56]M. R. Zirnbauer, J. Math. Phys. **37**, 4986 (1996).
[57]L. P. Gor'kov, O. N. Dorokhov, and F. V. Prigara, Zh. Eksp. Teor. Fiz. **84**, 1440 (1983) [Sov. Phys. JETP **57**, 838 (1983)].